

Pulse Image Processing Using Centripetal Autowaves

Jason M. Kinser and Chau Nguyen
The Institute for Biosciences, Bioinformatics, and Biotechnology
George Mason University, MSN 4E3
Email: jkinser@gmu.edu

Abstract

The mammalian visual cortex has presented unique visual processing algorithms. These systems rely on spiking neural networks that are coupled leaky-integrators. It has been proposed that the visual system converts 2D images into 1D signatures. So far, efforts to create digital algorithms have been thwarted by interference amongst objects in the input space. Here the marriage of curvature flow with pulse image processing creates a new system in which the expanding autowaves of individual objects in an input scene do not interfere. Thus, it becomes possible to identify multiple objects in a scene solely through the 1D signature.

Keywords: Centripetal autowaves, unified cortical model, curvature flow, recognition.

1. INTRODUCTION

Recently, several models of the mammalian visual cortex have been proposed¹. These models produce a set of pulse images (binary elements) from a static input. A digital model, the Pulse-Coupled Neural Network (PCNN)² proposed using these pulse images to create a signature that could be used for object recognition.

While the PCNN signatures were shown to be excellent discriminators for isolated objects they have not been shown to be discriminators of objects that are embedded in a background. The problem is that the target object and the background objects interfere thus drastically altering the target signature.

This paper will consider the construct of the cortical models and the reason for the interference. Then this paper will propose a solution to the interference problem and construct an cortical model that uses centripetal autowaves to extract a similar target signature without the problems of interference.

2. CORTICAL THEORY

As stated above there are several cortical models that have been proposed. They do have a common mathematical foundation and for the purposes here all algorithms behave similarly. Therefore, the algorithm used here is a unified cortical model (UCM) that contains only the similarities from the different cortical models. These similarities are that each neuron has at least two memories that are leaky integrators. These two memories are linked. Furthermore, neurons communicate with close neighbors only.

The UCM neuron has two memories F and T . F is the neuronal potential and T is the dynamic threshold. To feed the network the input image is sent to a 2D array of neurons (one neuron per pixel). Thus, the UCM is described as matrix equations,

$$\mathbf{F}[n + 1] = f\mathbf{F}[n] + \mathbf{S} + \mathbf{W} \mathbf{Y}[n] , \quad (1)$$

$$\mathbf{Y}[n + 1] = \mathbf{F}[n + 1] > \mathbf{T}[n] , \quad (2)$$

$$\mathbf{T}[n + 1] = g\mathbf{T}[n] + h\mathbf{Y}[n + 1] , \quad (3)$$

where \mathbf{S} is the input, \mathbf{W} is a local positive synaptic connection tensor, \mathbf{F} and \mathbf{T} are the arrays of the neuron memories, \mathbf{Y} is the array of neuron outputs, f and g are scalars less than 1.0, and h is a large scalar. The second equation is a condensed notation that basically sets $Y_{ij}=1$ if $F_{ij} > T_{ij}$. This system receives an input \mathbf{S} and iterates these equations until the user stops it. Each iteration produces an output \mathbf{Y} which is an image of binary pixels. An example is shown in figure 1.



Figure 1a. An original input image. Figures 1b-d are three pulse images from the UCM.

The usefulness of the UCM and other cortical models is that the pulse images provide natural segments of the input image. This property has been used in a variety of applications³.

Johnson² proposed that the pulse images could be used to generate the image signature via,

$$G_n = \prod_{ij} Y_{ij}[n]. \quad (4)$$

While there is strong evidence that images are converted to signatures⁴ the mechanism used here is not claimed to be representative of the biological system.

3. SIGNATURE DISCRIMINATION

The signatures for a set of images were compared to determine the feasibility of recognition and discrimination. The database consisted of isolated objects (no background) and varied in size. The signature for each was computed and the average of all signatures was removed from each signature. The signatures were compared by normalized inner products. Thus, the result of a signature compared to itself would be 1.0. Deviations from this exact match would present a lower comparison result.

The UCM was run for 50 iterations and a typical signature is shown in figure 2. The neurons have a cyclical behavior which accounts for the large frequency components of the signatures.

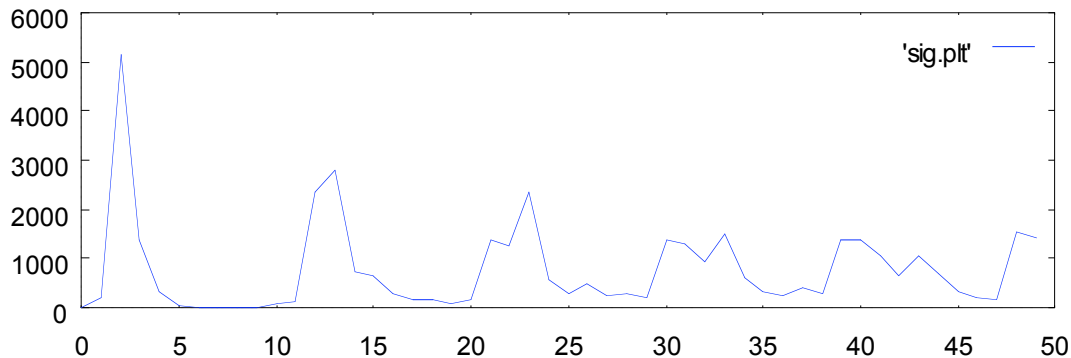


Figure 2. A typical signature.

Interestingly, only one pair of images from the set scored about 0.9 and those two images are shown in figure 3. In the first order sense these images are not similar. However, there are higher order similarities. Both images have a body and five extensions from the main body. The UCM is rotationally invariant as will be seen later. Thus, the system is seen extracting more syntactical information than statistical.



Figure 3. The best match from the database.

Thus, the signatures were discriminatory and could be separated by their signatures.

In order to demonstrate the recognition ability of the signatures one of the inputs was altered by several different means and the signature of the altered image was compared to the database of signatures.

3.1. Rotation Test

The rotation test was to simply rotate the input and create a new signature. The rotational invariance of these algorithms has already been noted in ref. 2. Thus, it is expected that little alteration to the signature is created by rotating the image.

The control portion of this experiment is to compare the signature of the image not rotated to the other signatures.

The results of the scaled inner products were

$$S = (1.0, -0.022, -0.289, 0.678, 0.084, 0.495, -0.601, 0.535, -0.496, 0.013).$$

It is obvious that the first image was the one used for this test. This image was certainly not confused with others in the database.

The test then rotated the input image and computed a new G. This new G was compared to the database of signatures. All tests run were very similar to the following example of a rotation of 49 degrees,

$$T = (0.999, -0.023, -0.294, 0.682, 0.090, 0.500, -0.605, 0.539, -0.498, 0.020).$$

As can be seen there was very little difference in the output. The total error of this system computed by

$$E = \sum_i |S_i - T_i|, \quad (5)$$

where \mathbf{S} is the vector of comparisons from the control and \mathbf{T} is the vector of comparisons from the test. The total error for this test was miniscule at 0.004.

3.2. Scale Test

The next test was to change the scale of the input image. The results were more sensitive than the rotation test, but the system could accept some scale change. The control test produced the same result

$$S = (1.0, -0.022, -0.289, 0.678, 0.084, 0.495, -0.601, 0.535, -0.496, 0.013).$$

When the input was reduced by a factor 0.9 the resultant comparisons were

$$(0.974, -0.159, -0.480, 0.818, 0.281, 0.677, -0.703, 0.649, -0.477, 0.184)$$

and the error was 0.128. Similarly, the error for a scale factor of 0.8 was 0.238.

While the change in the signature was noticeable it should be noted that discrimination was not compromised.

3.3. Illumination Test

The third test was to change the overall intensity of the input image. Again the signatures were altered by this change in the input. This is due to the fact that the UCM is operating in discrete time. Models in analog time have shown a truer invariance to illumination but are more difficult to manage.

The error for an illumination degradation by a factor of 0.9 was 0.093, by a factor of 0.8 was 0.169, and by a factor of 0.7 was 0.277.

3.4. Noise Test

The final test was to add random noise to the input. Cortical models have had a tendency to desynchronize⁵ and noise accelerates this effect. For an additive noise level of 5% of the maximum intensity value the error was 0.125 and for a noise level of 10% the error was 0.218.

3.5. Summary

While altering the quality of the image does alter the signatures of the images the decay of the signatures did not sacrifice the ability to discriminate between individual images. Thus, a generalization to these images is possible.

4. SIGNATURE INTERFERENCE

The images used above were isolated objects in that they had no background. The UCM algorithm is quite ignorant as to which pixels are on-target. Thus, when a background is present the off-target pixels will pulse as well. The intra-neuron communications create autowaves that present an interference problem. Interference was been notoriously destructive to the ability to discriminate using signatures.

4.1. Autowaves

Autowaves are waves that propagate but do not reflect or refract⁶. Thus, when two autowaves collide the wavefronts are annihilated along the intersection. Figure 4 displays an input of two circles. The subsequent images depict the autowave propagation from these two circles.

The neurons in the UCM (as well as the other models) communicate with their close neighbors. Positive connections will provide encouragement for neighboring neurons to pulse. When neighbors pulse they in turn encourage their neighbors to pulse. However, the large value of h in the UCM prevents neurons from pulsing in successive iterations. Thus, a wave of pulsing activity is established and this wave behaves as an autowave.

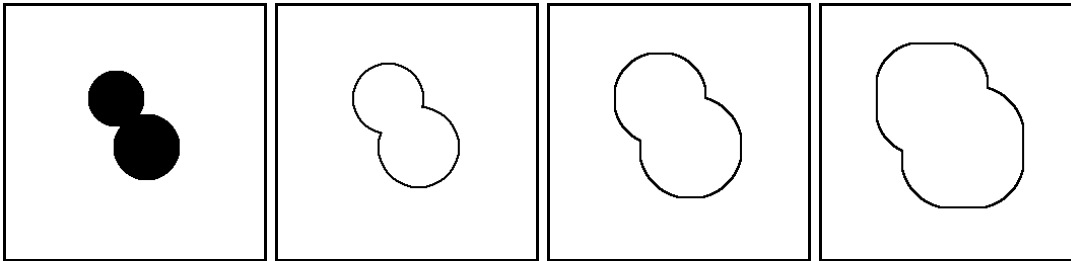


Figure 4. An input of two circles and the autowave propagation.

4.2. Interference

These expanding autowaves are the root cause of interference. The autowaves expanding from non-target objects will alter the autowaves emanating from target objects. If the non-target object is brighter it will pulse earlier than the target object autowaves. Thus, the pulsing behavior of on-target pixels can be seriously altered by the presence of other objects.



Figure 5. A target pasted on a background.

An image was created by pasting a target (a flower) on a background (figure 5). The target was intentionally made to be darker than the background to amplify the interference effect. The UCM was ran on both an image with the background and an image without the background. Only the pixels on-target were considered in creating the signatures shown in figure 6. The practice of including only on-target pixels is not possible for discrimination, but it does isolate the interference effects.

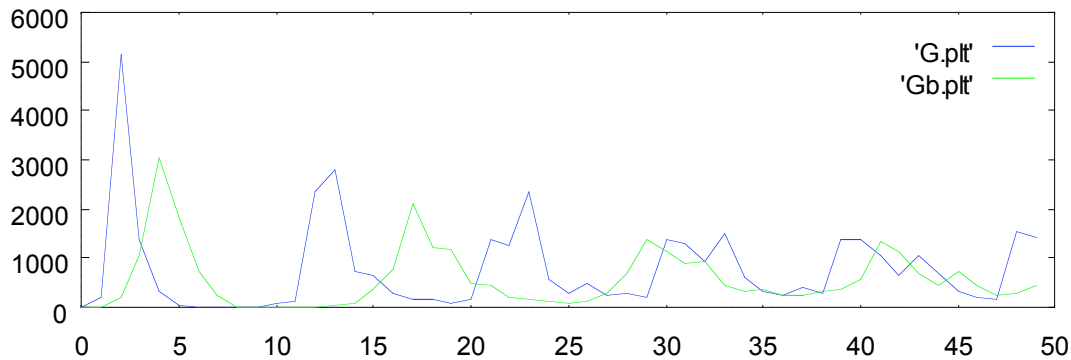


Figure 6. Plots of a signature from an image without the background ('G.plt') and an image with the background ('Gb.plt').

As can be seen the effects of the presence of a background are dramatic and recognition using these signatures is quite difficult.

4.3. Centripetal Autowave UCM

The solution to this problem is to alter the behavior of the autowaves since they are the chief instrument in creating the interference. However, the autowaves are also very important to the ability of the UCM to extract image segments.

4.3.1. Curvature Flow

Another type of wave propagation is that of curvature flow⁷. In this scenario the waves propagate towards the centripetal vectors that are perpendicular to the wavefront. Basically, they propagate towards local center of curvatures. For solid objects the curvature flows will become a circle and then collapse to a point⁸. (There is an ongoing debate as to the validity of this statement in dimensions higher than two.) Such propagation from ref. 7 is shown in figure 7.



Figure 7. Curvature flow propagation⁷.

4.3.2. Centripetal Autowaves

Centripetal autowaves are autowaves that follow the mechanics of curvature flow. Thus, when a segment pulses its autowaves will become a circle and then collapse. It does not propagate outwards as does the traditional autowave. The advantageous result is that autowaves developed from two neighboring objects will have far less interference. The centripetal autowave signatures of the same two images used to generate the results in figure 6 are shown in figure 8.

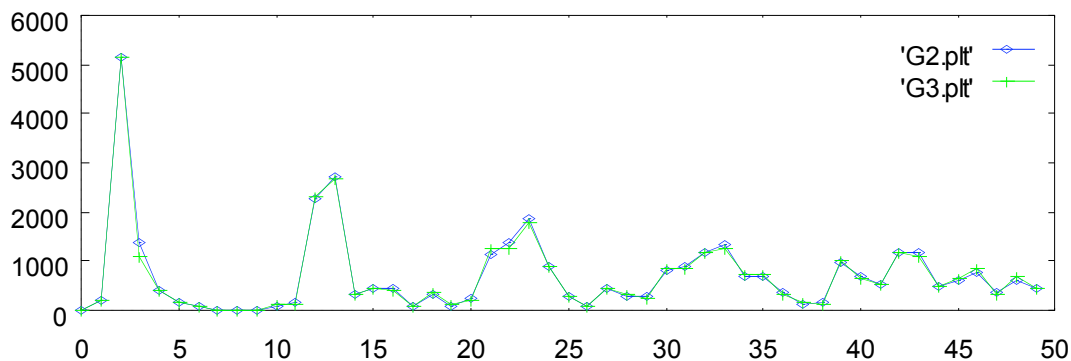


Figure 8. Signatures from an image without a background ('G2.plt') and with a background ('G3.plt') using the centripetal autowave model.

It is easy to see that the background no longer interferes with the object signature. Thus, discrimination becomes possible.

4.3.3. The Model

To accomplish the centripetal autowave propagation the first equation in the UCM is modified. The autowaves are born from the $\mathbf{W} \quad \mathbf{Y}$ term. This term is removed and replaced with $A(\mathbf{Y})$ which is a curvature flow algorithm⁷. However, this computation is somewhat complicated and a faster (but less accurate) was employed.

This faster system relied on the fact that the segments had binary elements and were solid. Operating on a such a segment with a smoothing operator will provide the necessary information. Consider the region marked by '1' in figure 9. This region is off-target yet is surrounded by on-target regions. Region '2' on the other hand is off-target and surrounded mostly by off-target pixels. After the smoothing operation the pixels in region 1 will have a higher value than the pixels in region 2. This relationship between concavity and smoothing holds for on-target pixels but in the opposite fashion.

Thus, simple thresholds (separate for on-target and off-target pixels) are used to indicate which direction the centripetal autowave must propagate. For example, pixels off-target with values above threshold should encourage the wavefront to move in that direction. Likewise, pixels on-target with a value below a different threshold should encourage the wavefront to move in that direction.

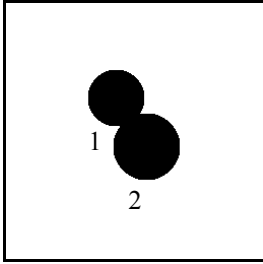


Figure 9. Region 1 and 2 are used to depict regions of different concavity.

Thus $A(\mathbf{Y})$ is the new segmented image that has moved the wavefronts in a centripetal fashion. The net result is that the autowaves do not interfere and the on-target neurons behave quite similar independent of the presence or absence of a background.

4.4. Invariance Performance

Since such a drastic alteration to the algorithm was created it becomes necessary to test the performance to variances to the input image. The rotation of the input image again had very little effect on the output. Following the similar format of the UCM test the rotate error was miniscule. Since error for no rotation was 0.0634 (comparing the centripetal autowave signature to the same database used above). The error for a rotation of 49 degrees was 0.0726. Similar small errors were seen for all rotations.

The scale, illumination, and noise tests also behaved in a similar manner to the above tests. For example, samples of the scale test are (scale=1.0, error=0.0634) and (scale=0.9, error=0.182).

5. SUMMARY

Centripetal autowaves are useful in isolating the effects of separate objects within a unified cortical model yet the segmentation of the algorithm is not compromised. This paper presents such a modification and demonstrates that the image signatures extracted from the unified cortical model are highly invariant to the presence of a background. This is an important step to the use of image signatures in object identification.

ACKNOWLEDGMENTS

This project was supported by a grant from the National Imagery and Mapping Agency University Research Initiative.

REFERENCES

1. For a review of several cortical models see: J. M. Kinser, "Hardware: Basic Requirements for Implementation", Proc. Of SPIE, **3728**, Stockholm, June 1998, 222-229.
2. J. L. Johnson, "Pulse-coupled neural nets: translation, rotation, scale, distortion, and intensity signal invariances for images", Appl. Opt. **33**(26), 6239-6253 (1994).
3. T. Lindblad & J. Kinser, Image Processing using Pulsed Coupled Neural Networks, Springer-Verlag, London, 1998.
4. J. W. McClurkin, J. A. Zarbock, L. M. Optican, "Temporal Codes for Colors, Patterns and Memories" Cerebral Cortex, v10, A.Peters and K.Rockland eds., Plenum Press, NY, (1994), 443-467.
5. O. Parodi, P. Combe, J-C. Ducom, "Temporal Encoding in Vision: Coding by Spike Arrival Times Leads to Oscillations in the Case of Moving Targets", Biol. Cybern. **74**, 497-509 (1996).
6. O. A. Mornev, "Elements of the 'Optics' of Autowaves" in Self-Organization Autowaves and Structures far from Equilibrium, V. I. Krirsky ed., Springer-Verlag, pp111-118 (1984).
7. R. Malladi, J. A. Sethian, "Level Set Methods for Curvature Flow, Image Enhancement, and Shape Recovery in Medical Images", Proc. of Conf. on Visualization and Mathematics, June 1995, Springer-Verlag, 329-345, (1995).
8. M. A. Grayson, "The Heat Equation Shrinks Embedded Plane Curves to Round Points", J. Differential Geomery, **26**, 285-314, (1987).